PERGAMON

Chaos, Solitons and Fractals 12 (2001) 1459–1471

CHAOS
SOLITONS & FRACTALS

www.elsevier.nl/locate/chaos

Effect of the potential shape and of a Brownian particle mass on noise-induced transport

Polina S. Landa [a], Alexey Zaikin [b,*], Lutz Shimansky-Geier [c]

[a] Department of Physics, Lomonosov Moscow State University, 119899 Moscow, Russian Federation
[b] Institute of Physics, University of Potsdam, Am Neuen Palais 10, 14469 Potsdam, Germany
[c] Humboldt-University at Berlin, Invalidenstr. 110, D-10115 Berlin, Germany

Accepted 23 May 2000

Abstract

The noise-induced transport of a Brownian particle with regard to its mass is considered. The results of approximate analytical calculations for the averaged probability flux in periodic ratchet-like potentials are presented. The influence of the potential shape on the mean particle velocity is traced. In the case of sufficiently small particle mass, it is shown that with increase in mass the reversal of flux is possible.

1. Introduction

In recent years, phenomena of noise-induced transport for Brownian particles have been attracting considerable interest of many scientists, for the most part in the context of different biological and chemical problems (see, for example, [1–10]). A physical experiment demonstrating the possibility of such transport in a ratchet-like potential field created by laser beam is described in [11]. In [12], it was experimentally shown that directed motion of a particle can be induced merely by turning on and off a periodic asymmetric potential (more recently, this phenomenon became known as a *flashing ratchet*). Similar experiments are also presented in [13].

Systems in which noise-induced transport occurs are often called stochastic ratchets by analogy with mechanical device 'ratchet-and-pawl' described and considered by Feynman [14].

In the last few years much attention has been concentrated on the problem associated with the separation of particles of different mass and size. In this connection, studies of different models giving flux reversals as the system parameters change are very important [10,15–18]. Below, we show analytically by an example of a special shape of the potential that under certain conditions flux reversal is possible with increasing intensity of noise or particle mass.

2. One-dimensional motion of a light Brownian particle in a viscous medium under a slow periodic force

2.1. The case of a saw-tooth potential

Here, we consider the case when viscous friction in the medium is sufficiently large and mass of the particle is sufficiently small, that the motion of the particle can be described approximately by the equation

* Corresponding author.

0960-0779/01/$ - see front matter
PII: S 0 9 6 0 - 0 7 7 9 (0 0) 0 0 1 1 9 - 3

$$\dot{x} + f(x) = \varphi(t) + \xi(t), \tag{1}$$

where

$$f(x) = \begin{cases} a_1 & \text{for } nL < x < nL + x_1, \\ -a_2 & \text{for } nL - x_2 < x < nL, \end{cases} \tag{2}$$

is a function corresponding to a periodic saw-tooth potential that is shown in Fig. 1, $n = 0, \pm 1, \pm 2, \ldots,$ $L = x_1 + x_2$ the period of the function $f(x)$, $\varphi(t) = B\cos\omega t$ the small periodic force, and $\xi(t)$ is white noise of intensity K imitating thermal fluctuations. It is easily shown that, in the absence of the force $\varphi(t)$ and of noise $\xi(t)$, the points $x = nL$ and $x = nL + x_1 = (n+1)L - x_2$ correspond to stable and unstable equilibrium states, respectively. If noise is present, then transitions from one stable state to another can occur. Directional motion of the particle will take place if the probabilities of transitions in opposite directions are different.

The Fokker–Planck equation associated with Eq. (1) is

$$\frac{\partial w}{\partial t} = -\frac{\partial}{\partial x}((\varphi(t) - f(x))w(x,t)) + \frac{K}{2}\frac{\partial^2 w(x,t)}{\partial x^2}. \tag{3}$$

Since $f(x)$ is a periodic function of x, $w(x,t)$ is also a periodic function of x. Thus, Eq. (3) only needs to be solved within the interval from $-x_2$ to x_1.

It is easily shown (see, for example, [19]) that the statistical average of the particle velocity $\dot{x}$, which determines the directional drift, is determined by the relationship

$$\langle \dot{x} \rangle = \int_{-x_2}^{x_1} G(x,t)\,\mathrm{d}x, \tag{4}$$

where

$$G(x,t) = -\frac{K}{2}\frac{\partial w(x,t)}{\partial x} + F(x,t)w(x,t) \tag{5}$$

can be treated as the instantaneous probability flux, $F(x,t) = \varphi(t) - f(x)$. Averaging (4) over time we have

$$\overline{\langle \dot{x} \rangle} = \int_{-x_2}^{x_1} \overline{G(x,t)}\,\mathrm{d}x, \tag{6}$$

where

$$\overline{G(x,t)} = \lim_{T\to\infty}\frac{1}{T}\int_0^T G(x,t)\,\mathrm{d}t.$$

So, the mean particle velocity, i.e., its net diffusive drift, is proportional to the probability flux averaged both over space and over time.

If the frequency ω is sufficiently small, we can use for solving the Fokker–Planck equation a quasi-stationary approximation (such an approximation they often call adiabatic one [20]). In this approximation, we obtain the following equation for $w_0(x,\varphi)$:

$$\frac{K}{2}\frac{\partial w_0(x,\varphi)}{\partial x} - (\varphi - f(x))w_0(x,\varphi) = -G_0(\varphi), \tag{7}$$

where $G_0(\varphi)$ is the probability flux. Solving Eq. (7) with account taken of (2) we find

$$w_0(x,\varphi) = \begin{cases} \left(C_0(\varphi) - \frac{G_0(\varphi)}{q_1}\right)\exp\left(\frac{2q_1 x}{K}\right) + \frac{G_0(\varphi)}{q_1} & \text{for } 0 \leqslant x \leqslant x_1, \\ \left(C_0(\varphi) - \frac{G_0(\varphi)}{q_2}\right)\exp\left(\frac{2q_2 x}{K}\right) + \frac{G_0(\varphi)}{q_2} & \text{for } -x_2 \leqslant x \leqslant 0, \end{cases} \tag{8}$$

where

$$q_{1,2} = \varphi \mp a_{1,2}, \tag{9}$$

and $C_0(\varphi)$ is an arbitrary function of φ. From the periodicity condition of the function $w_0(x, \varphi)$ we find the relation between $G_0(\varphi)$ and $C_0(\varphi) : C_0(\varphi) = Q(\varphi)G_0(\varphi)$, where

$$Q(\varphi) = \frac{1}{q_1 q_2} \frac{q_2 \exp(2U_0\varphi/Ka_1) - q_1 \exp(-2U_0\varphi/Ka_2) - (q_2 - q_1)\exp(2U_0/K)}{\exp(2U_0\varphi/Ka_1) - \exp(-2U_0\varphi/Ka_2)} \tag{10}$$

and $U_0 = a_1 x_1 = a_2 x_2$ is the height of the potential barrier. The probability flux $G_0(\varphi)$ can be found from the normalization condition for the probability density $w_0(x, \varphi)$. In so doing we obtain

$$\begin{aligned} G_0^{-1}(\varphi) = {} & U_0\left(\frac{1}{a_1 q_1} + \frac{1}{a_2 q_2}\right) + \frac{K(a_1 + a_2)^2}{2q_1^2 q_2^2} \exp\left(-\frac{2U_0}{K}\right) \\ & \times \frac{(\exp(2U_0\varphi/Ka_1) - \exp(2U_0/K))(\exp(-2U_0\varphi/Ka_2) - \exp(2U_0/K))}{\exp(2U_0\varphi/Ka_1) - \exp(-2U_0\varphi/Ka_2)}. \end{aligned} \tag{11}$$

In the most interesting case when φ is sufficiently small, namely when

$$\max \varphi \ll \frac{a_1 a_2}{a_2 - a_1} \min\left(1, \frac{K}{U_0}\right), \tag{12}$$

we find

$$G_0(\varphi) = G_{01}(\varphi) + G_{02}(\varphi)^2 + \cdots, \tag{13}$$

where

$$\begin{aligned} G_{01} &= \frac{U_0 a_1 a_2}{K^2(a_1 + a_2)\sinh^2(U_0/K)}, \\ G_{02} &= G_{01}\frac{a_2 - a_1}{a_1 a_2}\left(\frac{U_0^2}{K^2\sinh^2(U_0/K)} + \frac{U_0}{K\tanh(U_0/K)} - 2\right). \end{aligned} \tag{14}$$

Since $\overline{\varphi} = 0$ we obtain from (14) and (6)

$$\overline{\langle \dot{x} \rangle} \approx \frac{U_0^2(a_2 - a_1)B^2}{2K^2 a_1 a_2 \sinh^2(U_0/K)}\left(\frac{U_0^2}{K^2\sinh^2(U_0/K)} + \frac{U_0}{K\tanh(U_0/K)} - 2\right), \tag{15}$$

i.e., the particle moves in the direction of the slower rate of potential change. It is easy to verify that, in the absence of noise ($K = 0$), transport of the particle cannot occur.

Examples of the dependences of $\overline{\langle \dot{x} \rangle}/B^2$ on K/U_0 described by formulas (6) and (11) are shown in Fig. 2 for a number of values of B. We see that these dependences are of radically different kinds for $B < \min(a_1, a_2)$ and $B > \min(a_1, a_2)$. In the first case, these dependences have a maximum at a certain value of K/U_0 that is the smaller, the greater is B. For $K/U_0 \to 0$, i.e., in the absence of the thermal fluctations, $\overline{\langle \dot{x} \rangle}/B^2 \to 0$. In the second case, $\overline{\langle \dot{x} \rangle}/B^2$ tends to a certain finite value as $K/U_0 \to 0$, which can be calculated from the theory of vibrational transport [10,21]. For $B < 0.5$ the dependences found are almost coincident with those described by the approximate formula (15). In this case, the averaged particle velocity is maximal for $K/U_0 \approx 0.43$. If the ratio K/U_0 is either very small or very large, noise-induced transport is not feasible.

We note that a similar problem was solved numerically in [22] by using the so-called matrix continued fraction technique. It was shown that, for low frequencies, the numerical results coincide with the quasi-stationary approximation. But for high frequencies the results obtained were radically different, for example, a reversal of the probability flux over certain ranges of K/U_0 and B was detected.

2.2. The effect of the potential shape

It is interesting to find how the shape of the potential influences noise-induced transport. In the case of arbitrary periodic potential $U(x)$ a quasi-stationary solution of the Fokker–Planck equation (3) is

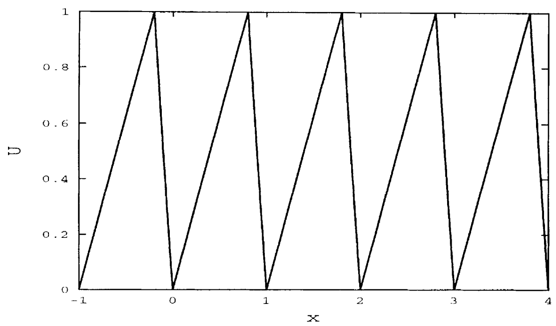

1

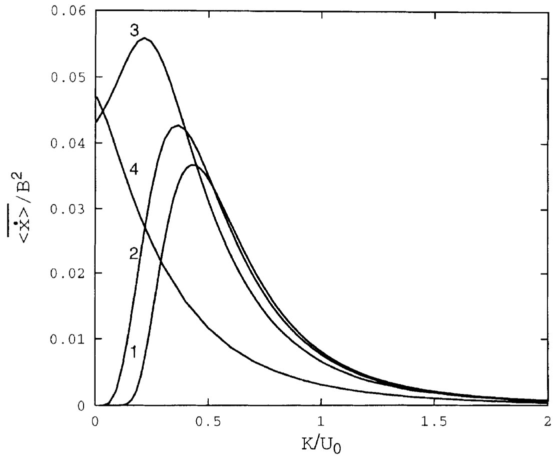

2

Fig. 1. An example of a saw-tooth potential $U(x)$.

Fig. 2. Dependence of $\overline{\langle\dot{x}\rangle}/B^2$ on K/U_0 as described by Eqs. (6) and (11) for $a_1 = 1.25, a_2 = 5, x_1 = 0.8, x_2 = 0.2$, and: $B = 0.1$ (curve 1); $B = 1$ (curve 2); $B = 2$ (curve 3); and $B = 5$ (curve 4).

$$w(x,t) = \left[C(\varphi(t)) - \frac{2G(\varphi(t))}{K}\int_0^x \exp\left(\frac{2(U(x') - \varphi(t)x')}{K}\right) \mathrm{d}x'\right] \exp\left(-\frac{2(U(x) - \varphi(t)x)}{K}\right), \tag{16}$$

where $C(\varphi(t))$ and $G(\varphi(t))$ are arbitrary functions of t. From the periodicity condition of the function $w(x,t)$ we find the relationship between $C(\varphi)$ and $G(\varphi)$

$$C(\varphi) = \frac{2G(\varphi)I_1(\varphi)}{K}\left[1 - \exp\left(-\frac{2L\varphi}{K}\right)\right]^{-1}, \tag{17}$$

where L is the period of the functions $f(x)$ and $U(x)$,

$$I_1(\varphi) = \int_0^L \exp\left(\frac{2(U(x) - \varphi x)}{K}\right) \mathrm{d}x. \tag{18}$$

Taking account of (17) and from the normalization condition we determine $G(\varphi)$

$$G(\varphi) = \frac{K}{2}\left\{I_1(\varphi)I_2(\varphi)\left[1 - \exp\left(-\frac{2L\varphi}{K}\right)\right]^{-1} - I_3(\varphi)\right\}^{-1}, \tag{19}$$

where

$$\begin{aligned} I_2(\varphi) &= \int_0^L \exp\left(-\frac{2(U(x) - \varphi x)}{K}\right) \mathrm{d}x, \\ I_3(\varphi) &= \int_0^L \int_0^x \exp\left(-\frac{2(U(x') - U(x) - \varphi(x' - x))}{K}\right) \mathrm{d}x'\mathrm{d}x. \end{aligned} \tag{20}$$

If the amplitude B satisfies to the condition

$$LB \ll K, \tag{21}$$

we find from (19)

$$G(\varphi) \approx G_{01}\varphi + G_{02}\varphi^2, \quad I_1(\varphi) \approx I_{10} - I_{11}\varphi, \quad I_2(\varphi) \approx I_{20} + I_{21}\varphi, \quad I_3(\varphi) \approx I_{30}, \tag{22}$$

where

$$G_{01} = \frac{L}{I_{10}I_{20}}, \quad G_{02} = G_{01}\left(\frac{I_{11}}{I_{10}} - \frac{I_{21}}{I_{20}} - \frac{L}{K}\left(1 - \frac{2I_{30}}{I_{10}I_{20}}\right)\right),$$
$$I_{10} = \int_0^L \exp\left(\frac{2U(x)}{K}\right) dx, \quad I_{20} = \int_0^L \exp\left(-\frac{2U(x)}{K}\right) dx, \tag{23}$$
$$I_{11} = \frac{2}{K}\int_0^L x\exp\left(\frac{2U(x)}{K}\right) dx, \quad I_{21} = \frac{2}{K}\int_0^L x\exp\left(-\frac{2U(x)}{K}\right) dx.$$

By substituting (22) into (6) we obtain

$$\overline{\langle \dot{x} \rangle} \approx \frac{L^2B^2}{2I_{10}I_{20}}\left(\frac{I_{11}}{I_{10}} - \frac{I_{21}}{I_{20}} - \frac{L}{K}\left(1 - \frac{2I_{30}}{I_{10}I_{20}}\right)\right). \tag{24}$$

As the first example, we set the function $f(x)$ proportional to the first two terms of the Fourier series for $f(x)$ described by (2), viz

$$f(x) = \sum_{n=1}^{N} \frac{1.1}{n\pi}\left((a_1 + a_2)\sin\frac{2\pi n(x + x_0)}{L} - a_1 \sin\frac{2\pi n(x + x_0 - x_1)}{L} - a_2 \sin\frac{2\pi n(x + x_0 + x_2)}{L}\right), \tag{25}$$

where x_0 is chosen so that $U(0) = 0$. Plots of the functions $U(x) = \int_0^x f(x)\,dx$ and $f(x)$ for $x_1 = 0.8$, $x_2 = 0.2$, $x_0 = 0.075$ and $N = 2$ are shown in Fig. 3(a).

As the second example, we take the function $f(x)$ associated with a saw-tooth potential with smoothed edges. This function and the corresponding potential $U(x)$ are described by the following expressions:

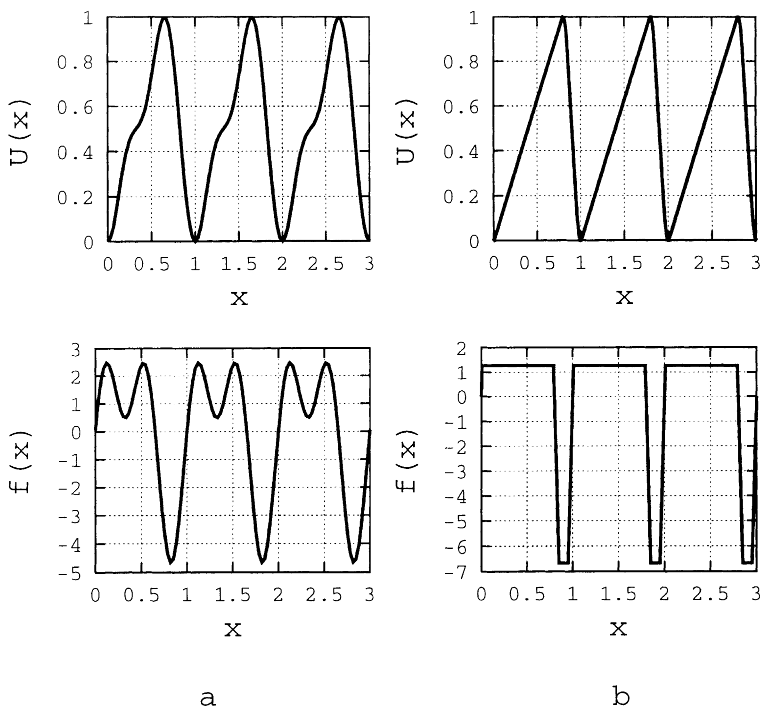

Fig. 3. Plots of the functions $U(x) = \int_0^x f(x)\,dx$ and $f(x)$ as determined by equations: (a) (25) for $a_1 = 1.25, a_2 = 5, x_1 = 0.8, x_2 = 0.2$, and $x_0 = 0.075$; (b) (26) and (27) for $x_1 = 0.8$, $x_2 = 0.2$, and $l_2 = 0.05$ ($l_1 = 0.015, a_1 \approx 1.27, a_2 \approx 6.67$, and $b \approx 133.33$).

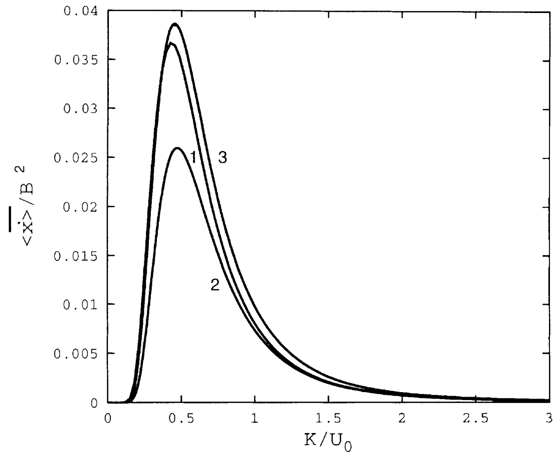

Fig. 4. Dependence of $\overline{\langle \dot{x} \rangle}/B^2$ on K/U_0 for $f(x)$ described by (2) (curve 1), (25) with $N = 2$ (curve 2), and (27) (curve 3), for the same values of the parameters as in Fig. 3.

$$f(x) = \begin{cases} bx & \text{for } 0 \leqslant x \leqslant l_1, \\ a_1 & \text{for } l_1 \leqslant x \leqslant x_1 - l_1, \\ a_1 - b(x - x_1 + l_1) & \text{for } x_1 - l_1 \leqslant x \leqslant x_1 + l_2, \\ -a_2 & \text{for } x_1 + l_2 \leqslant x \leqslant L - l_2, \\ -a_2 + b(x - L + l_2) & \text{for } L - l_2 \leqslant x \leqslant L, \end{cases} \tag{26}$$

$$U(x) = \begin{cases} \frac{bx^2}{2} & \text{for } 0 \leqslant x \leqslant l_1, \\ a_1\left(x - \frac{l_1}{2}\right) & \text{for } l_1 \leqslant x \leqslant x_1 - l_1, \\ 1 - \frac{b(x-x_1)^2}{2} & \text{for } x_1 - l_1 \leqslant x \leqslant x_1 + l_2, \\ 1 - a_2\left(x - x_1 - \frac{l_2}{2}\right) & \text{for } x_1 + l_2 \leqslant x \leqslant L - l_2, \\ \frac{b(x-L)^2}{2} & \text{for } L - l_2 \leqslant x \leqslant L, \end{cases} \tag{27}$$

where

$$a_1 = \frac{1}{x_1 - l_1}, \quad a_2 = \frac{1}{x_2 - l_2}, \quad l_1 = \frac{x_1}{2} - \sqrt{\frac{x_1^2}{4} - x_2 l_2 + l_2^2}, \quad b = \frac{a_2}{l_2},$$

$x_1 = 0.8,\ x_2 = 0.2,\ L = 1,\ l_2$ is a certain parameter that characterizes the extent to which the potential edges are smoothed. Plots of the functions $U(x)$ and $f(x)$ for $l_2 = 0.05$ ($l_1 \approx 0.0095,\ a_1 \approx 1.265,\ a_2 \approx 6.67$, and $b \approx 133.333$) are shown in Fig. 3(b).

For $f(x)$ described by the expressions (25) (for $a_1 = 1.25,\ a_2 = 5,\ x_1 = 0.8,\ x_2 = 0.2,\ N = 2$) and (27) (for the same values of x_1 and x_2 and $l_2 = 0.05$) the dependences of $\overline{\langle \dot{x} \rangle}/B^2$ on K/U_0 are illustrated in Fig. 4 (curves 2 and 3, respectively). For comparison, in the same figure the corresponding dependence for a non-smoothed saw-tooth potential is shown too (curve 1). We see that all of these dependences coincide in a qualitative sense but diverge quantitatively.

3. One-dimensional motion of a Brownian particle with consideration for its mass

We consider now the one-dimensional motion of a Brownian particle in a viscous medium described by the following equation:

$$\mu \ddot{x} + \dot{x} + f(x) = \varphi(t) + \xi(t), \tag{28}$$

where $\mu = m/\beta$, m the particle mass, β is the viscous friction factor. We assume that μ is sufficiently small, viz

$$\mu \ \max f'(x) \ll 1. \tag{29}$$

In this case, we can obtain an approximate one-dimensional Fokker–Planck equation for the probability density of the variable x, much as this was done by Stratonovich [23,24]. The derivation of such an equation is given in Appendix A. For $\mu = 0$ the equation found is the exact Fokker–Planck equation corresponding to the Langevin equation (1). It should be emphasized that the technique for derivation of the approximate one-dimensional Fokker–Planck equation is valid only if all derivaties of the function $f(x)$ are finite. This is why, strictly speaking, we cannot use it in the cases of the saw-tooth potential and of the smoothed saw-tooth potential.

Setting in Eq. (A.20) $\epsilon^2 = \mu$, taking into account that $F(x,t) = f(x) - \varphi(t)$, and retaining the terms up to the order 4, inclusive, with respect to μ, we find the following quasi-stationary solution of the equation for $w(x,\varphi)$:

$$\begin{aligned} w(x,\varphi) = {} & \exp\left(-\frac{2(U(x)-\varphi(t)x)}{K}\right)\left\{C(\varphi) - \frac{2G(\varphi)}{K}\int_0^x \left((1-\mu f'(x') - \mu^2\left[\frac{3K}{4}f'''(x)\right.\right.\right. \\ & \left. + 2F(x,t)f''(x) + (f'(x))^2\right] - \mu^3\left[\frac{29K^2}{48}f^{V}(x) + \frac{K}{8}\left(23F(x,t)f^{IV}(x) + 52f'(x)f'''(x)\right.\right. \\ & \left.\left. + 31(f''(x))^2\right) + \frac{7}{2}F^2(x,t)f'''(x) + 12F(x,t)f'(x)f''(x) + 2(f'(x))^3\right] - \mu^4\left[\frac{143K^3}{288}f^{VII}(x)\right. \\ & + \frac{K^2}{144}\left(485F(x,t)f^{VI}(x) + 1677f^{V}(x)f'(x) + 3081f^{IV}(x)f''(x) + 1820(f'''(x))^2\right) \\ & + \frac{K}{16}\left(123F^2(x,t)f^{V}(x) + 713F(x,t)f^{IV}(x)f'(x) + 1147F(x,t)f'''(x)f''(x) + 760f'''(x)(f'(x))^2\right. \\ & \left. + 919(f''(x))^2f'(x)\right) + \frac{71}{12}F^3(x,t)f^{IV}(x) + \frac{83}{2}F^2(x,t)f'''(x)f'(x) + \frac{129}{2}F(x,t)f''(x)(f'(x))^2 \\ & \left.\left.\left. + \frac{105}{4}F^2(x,t)(f''(x))^2 + 5(f'(x))^4\right]\right)\exp\left(\frac{2(U(x')-\varphi x')}{K}\right)\mathrm{d}x'\right\}, \end{aligned} \tag{30}$$

where $G(\varphi)$ is the probability flux at a fixed value of φ.

From the periodicity condition of the function $w(x,\varphi)$ we find the relationship between $C(\varphi)$ and $G(\varphi)$

$$\begin{aligned} C(\varphi) = {} & \frac{2G(\varphi)}{K}\left(I_1(\varphi) - \mu I_4(\varphi) - \mu^2(I_6(\varphi) - I_7(\varphi)\varphi) - \mu^3(I_{12}(\varphi) - I_{13}(\varphi)\varphi\right. \\ & \left. + I_{14}(\varphi)\varphi^2) - \mu^4(I_{18}(\varphi) - I_{19}(\varphi)\varphi + I_{20}(\varphi)\varphi^2 - I_{21}(\varphi)\varphi^3)\right)\left[1 - \exp\left(-\frac{2L\varphi}{K}\right)\right]^{-1}, \end{aligned} \tag{31}$$

where $I_1(\varphi)$ is determined by (18), and expressions for other integrals can be found in Appendix B.

Taking account of (30), we obtain from the normalization condition the following relation between $C(\varphi)$ and $G(\varphi)$:

$$\begin{aligned} CI_2 - \frac{2G}{K}&[I_3(\varphi) - \mu I_5(\varphi) - \mu^2(I_8(\varphi) - I_9(\varphi)\varphi) - \mu^3(I_{15}(\varphi) - I_{16}(\varphi)\varphi + I_{17}(\varphi)\varphi^2) \\ & - \mu^4(I_{22}(\varphi) - I_{23}(\varphi)\varphi + I_{24}(\varphi)\varphi^2 - I_{25}(\varphi)\varphi^3)] = 1, \end{aligned} \tag{32}$$

where $I_2(\varphi)$, $I_3(\varphi)$ are determined by (20), and other integrals can be found in Appendix B.

Substituting (31) into (32) we can find $G(\varphi)$. It can be written as

$$G(\varphi) = G_0(\varphi)\left(1 + \mu M_1(\varphi) + \mu^2 M_2(\varphi) + \mu^3 M_3(\varphi) + \mu^4 M_4(\varphi)\right), \tag{33}$$

where $G_0(\varphi)$ is determined by formula (19), and

$$
\begin{aligned}
M_1(\varphi) &= \frac{I_2(\varphi)I_4(\varphi) - I_5(\varphi)(1-\exp(-2L\varphi/K))}{I_1(\varphi)I_2(\varphi) - I_3(\varphi)(1-\exp(-2L\varphi/K))},\\
M_2(\varphi) &= M_1^2(\varphi) + \frac{I_2(\varphi)(I_6(\varphi) - I_7(\varphi)\varphi) - (I_8(\varphi) - I_9(\varphi)\varphi)(1-\exp(-2L\varphi/K))}{I_1(\varphi)I_2(\varphi) - I_3(\varphi)(1-\exp(-2L\varphi/K))},\\
M_3(\varphi) &= 2M_1(\varphi)M_2(\varphi) - M_1^3(\varphi) + \frac{I_2(\varphi)(I_{12}(\varphi) - I_{13}(\varphi)\varphi + I_{14}(\varphi)\varphi^2)}{I_1(\varphi)I_2(\varphi) - I_3(\varphi)(1-\exp(-2L\varphi/K))}\\
&\quad - \frac{(I_{15}(\varphi) - I_{16}(\varphi)\varphi + I_{17}(\varphi)\varphi^2)(1-\exp(-2L\varphi/K))}{I_1(\varphi)I_2(\varphi) - I_3(\varphi)(1-\exp(-2L\varphi/K))},\\
M_4(\varphi) &= M_1(\varphi)(2M_3(\varphi) - M_1(\varphi)M_2(\varphi)) + (M_2(\varphi) - M_1^2(\varphi))^2\\
&\quad + \frac{I_2(\varphi)(I_{18}(\varphi) - I_{19}(\varphi)\varphi + I_{20}(\varphi)\varphi^2 - I_{21}(\varphi)\varphi^3)}{I_1(\varphi)I_2(\varphi) - I_3(\varphi)(1-\exp(-2L\varphi/K))}\\
&\quad - \frac{(I_{22}(\varphi) - I_{23}(\varphi)\varphi + I_{24}(\varphi)\varphi^2 - I_{25}(\varphi)\varphi^3)(1-\exp(-2L\varphi/K))}{I_1(\varphi)I_2(\varphi) - I_3(\varphi)(1-\exp(-2L\varphi/K))}.
\end{aligned}
\tag{34}
$$

If φ is sufficiently small then in (33) we can retain only the terms of order of φ and φ^2. In so doing we can put $G_0(\varphi) = G_{01}\varphi + G_{02}\varphi^2$, where G_{01} and G_{02} are determined by (23), and

$$M_i(\varphi) = M_{i0} + M_{i1}\varphi \ (i = 1, 2, 3, 4).$$

For $\varphi(t) = B\cos\omega t$ we obtain

$$
\begin{aligned}
\overline{\langle\dot{x}\rangle} \approx \frac{B^2L}{2}[G_{02} &+ \mu(G_{01}M_{11} + G_{02}M_{10}) + \mu^2(G_{01}M_{21} + G_{02}M_{20})\\
&+ \mu^3(G_{01}M_{31} + G_{02}M_{30}) + \mu^4(G_{01}M_{41} + G_{02}M_{40})].
\end{aligned}
\tag{35}
$$

For $f(x)$ described by formula (25) the dependences of $\overline{\langle\dot{x}\rangle}/B^2$ on K/U_0 for $\mu = 0$ and $\mu = 0.005$ are shown in Fig. 5. We see that up to the fourth approximation the flux reversal does not occur for any values of K/U_0. Only in the fourth approximation, for moderately large values of $K/U_0 (K/U_0 > 5)$ it takes place.

It is evident that the dependence of the mean velocity of a particle on its mass can be used for the separation of particles of different masses. Examples of the dependences of $\overline{\langle\dot{x}\rangle}/B^2$ on μ for two values of K/U_0 calculated in the second, third, and fourth approximations are illustrated in Fig. 6. We see that the difference between the results is essential even for small $\mu\gamma$. The significant difference between the results, obtained in different approximations for $\mu > 0.002$, points to the fact that the series on the left-hand side of Eq. (A.19) converges only asymptotically. This is why the conclusion about the flux reversal calls for futher investigation.

We note that the results obtained coincide qualitatively with the corresponding results of [10], where a saw-tooth potential was considered.

4. Summary

In conclusion, our investigation of the influence of potential shape and particle mass on the particle transport in stochastic ratchet devices showed that the shape of potential causes only quantitative changes in the probability flux, whereas the increase of particle mass can lead to qualitative changes such as flux reversal. Since, according to our results, the flux reversal is found only in the fourth approximation with respect to mass, further investigations are required. We note that we obtained the flux reversal both with increase of noise intensity and with increase of particle mass.

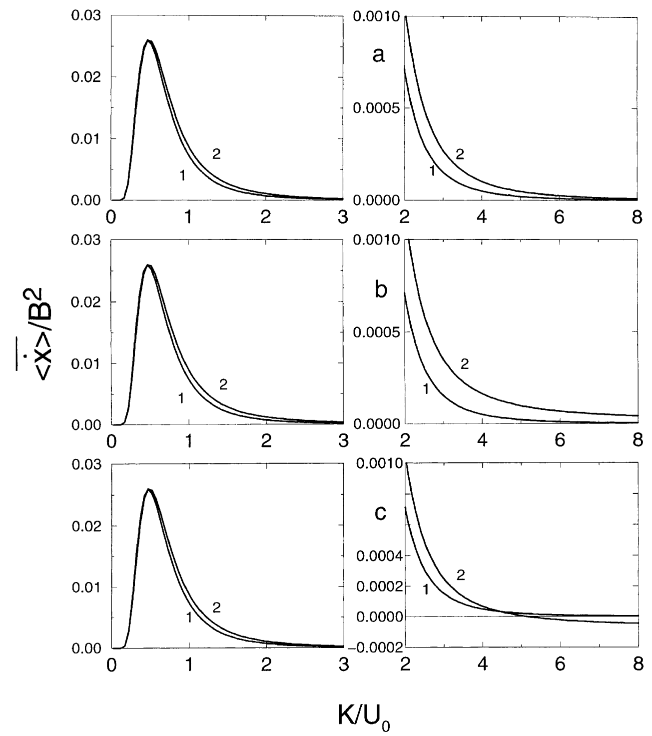

Fig. 5. The dependences of $\overline{\langle \dot{x} \rangle}/B^2$ on K/U_0 for $f(x)$ described by formula (25) for $\mu = 0$ and $\mu = 0.005$ (curves 1 and 2): (a) in the second approximation, (b) in the third approximation, (c) in the fourth approximation; the results in the range $0 \leqslant K/U_0 \leqslant 3$ (on the left), and the results in the range $2 \leqslant K/U_0 \leqslant 8$ (on the right).

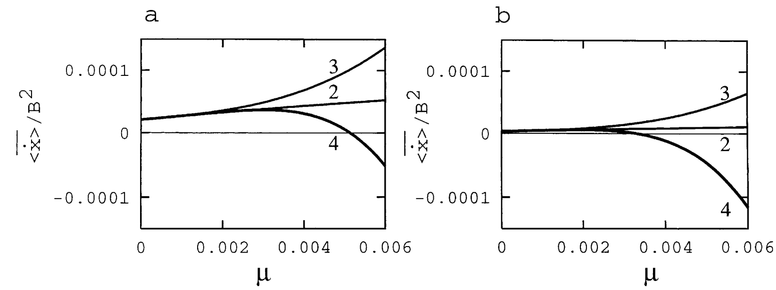

Fig. 6. The dependences of $\overline{\langle \dot{x} \rangle}/B^2$ on μ for (a) $K/U_0 = 5$ and (b) $K/U_0 = 8$. The results obtained in the second, third and fourth approximations with respect to μ are labelled 2, 3, and 4, respectively.

Acknowledgements

A.Z. acknowledges support from MPG.

Appendix A. Derivation of the approximate equation for the one-dimensional probability density

Let us consider an equation

$$\epsilon^2 \ddot{x} + \dot{x} + F(x) = \xi(t), \tag{A.1}$$

where $\xi(t)$ is white noise of zero mean and intensity K. Eq. (A.1) can be rewritten in the form of two equations of the first order

$$\epsilon\dot{x} = y, \quad \epsilon\dot{y} = -\frac{y}{\epsilon} - F(x) + \xi(x,t). \tag{A.2}$$

The two-dimensional Fokker–Planck equation associated with Eq. (A.2) is

$$\epsilon^2 \frac{\partial w(x,y,t)}{\partial t} = -\epsilon\left(y\frac{\partial w}{\partial x} - F(x)\frac{\partial w}{\partial y}\right) + \frac{\partial (yw)}{\partial y} + \frac{K}{2}\frac{\partial^2 w}{\partial y^2}. \tag{A.3}$$

Let us seek a solution of Eq. (A.3) in the form of the following expansion:

$$w(x,y,t) = \sum_{n=0}^{\infty} \epsilon^n w_n(x,t) Y_n(y), \tag{A.4}$$

where $Y_n(y)$ are the eigenfunctions of the boundary-value problem described by the equation

$$\frac{K}{2}\frac{\mathrm{d}^2 Y}{\mathrm{d}y^2} + \frac{\mathrm{d}(yY)}{\mathrm{d}y} + \lambda Y = 0 \tag{A.5}$$

with the boundary conditions $Y(\pm\infty) = 0$. As can be easily shown, the eigenvalues of this problem $\lambda_n = n$, where $n = 0, 1, 2 \ldots$, and the eigenfunctions can be expressed in terms of the Hermite polynomials $H_n(z)$ as

$$Y_n(y) = \frac{(-1)^n}{\sqrt{\pi K 2^n n!}} \mathrm{e}^{-y^2/K} H_n\left(\frac{y}{\sqrt{K}}\right). \tag{A.6}$$

Substituting into (A.6) the expression for the Hermite polynomial we obtain

$$Y_n(y) = \sqrt{\frac{K^{n-1}}{\pi 2^n n!}} \frac{\mathrm{d}^n}{\mathrm{d}y^n}\left(\mathrm{e}^{-y^2/K}\right). \tag{A.7}$$

It can be shown that the functions $Y_n(y)$ satisfy the following orthogonality and normalization conditions:

$$\int_{-\infty}^{\infty} \frac{Y_n(y) Y_m(y)}{Y_0(y)}\, \mathrm{d}y = \delta_{nm}. \tag{A.8}$$

We substitute (A.4) into Eq. (A.3) taking into account the following relationships: [1]

$$\frac{\mathrm{d}Y_n(y)}{\mathrm{d}y} = \sqrt{\frac{2(n+1)}{K}} Y_{n+1}(y), \quad yY_n(y) = -\sqrt{\frac{K}{2}}\left(\sqrt{n+1}\, Y_{n+1}(y) + \sqrt{n}\, Y_{n-1}(y)\right), \tag{A.9}$$

$$\frac{\mathrm{d}(yY_n(y))}{\mathrm{d}y} = -\left(\sqrt{(n+1)(n+2)}\, Y_{n+2}(y) + nY_n(y)\right).$$

As a result, we find

$$\epsilon^2 \sum_{n=0}^{\infty} \epsilon^n Y_n \frac{\partial w_n}{\partial t} = \sum_{n=0}^{\infty} \epsilon^n \left[\epsilon\sqrt{\frac{K}{2}}\left(\sqrt{n+1}\, Y_{n+1} + \sqrt{n}\, Y_{n-1}\right)\frac{\partial w_n}{\partial x} + \epsilon F(x)\sqrt{\frac{2(n+1)}{K}} Y_{n+1} w_n - nY_n w_n\right]. \tag{A.10}$$

Equating the terms of $Y_n(y)$ with the same subscripts, we obtain the following equations:

$$\epsilon^2 \frac{\partial w_n}{\partial t} = \sqrt{\frac{K}{2}}\left(\sqrt{n}\frac{\partial w_{n-1}}{\partial x} + \epsilon^2\sqrt{n+1}\frac{\partial w_{n+1}}{\partial x}\right) + F(x)\sqrt{\frac{2n}{K}} w_{n-1} - nw_n. \tag{A.11}$$

[1] These relationships follow from the properties of Hermite polynomials.

For $n \leqslant 4$ these equations are

$$\frac{\partial w_0}{\partial t} = \sqrt{\frac{K}{2}}\frac{\partial w_1}{\partial x}, \tag{A.12}$$

$$\epsilon^2\frac{\partial w_1}{\partial t} = \sqrt{\frac{K}{2}}\frac{\partial w_0}{\partial x} + \epsilon^2\sqrt{K}\frac{\partial w_2}{\partial x} + \sqrt{\frac{2}{K}}F(x)w_0 - w_1, \tag{A.13}$$

$$\epsilon^2\frac{\partial w_2}{\partial t} = \sqrt{K}\frac{\partial w_1}{\partial_x} + \epsilon^2\sqrt{\frac{3K}{2}}\frac{\partial w_3}{\partial x} + \frac{2}{\sqrt{K}}F(x)w_1 - 2w_2, \tag{A.14}$$

$$\epsilon^2\frac{\partial w_3}{\partial t} = \sqrt{\frac{3K}{2}}\frac{\partial w_2}{\partial x} + \epsilon^2\sqrt{2K}\frac{\partial w_4}{\partial x} + \sqrt{\frac{6}{K}}F(x)w_2 - 3w_3, \tag{A.15}$$

$$\epsilon^2\frac{\partial w_4}{\partial t} = \sqrt{2K}\frac{\partial w_3}{\partial x} + \epsilon^2\sqrt{\frac{5K}{2}}\frac{\partial w_5}{\partial x} + 2\sqrt{\frac{2}{K}}F(x)w_3 - 4w_4. \tag{A.16}$$

Putting in Eq. (A.11) $w_i = w_{i0} + \epsilon^2 w_{i1} + \epsilon^4 w_{i2} + \epsilon^6 w_{i3} + \cdots (i = 1, 2, 3, \ldots)$, we can find sequentially the functions $w_{10}, w_{11}, \ldots, w_{1n}, \ldots$ The calculations show that for $n \geqslant 1$ these functions can be expressed as

$$w_{1n} = \Phi_1^{(n)}\frac{\partial^{2n-2}w_{10}}{\partial x^{2n-2}} + \Phi_2^{(n)}\frac{\partial^{2n-3}w_{10}}{\partial x^{2n-3}} + \cdots + \Phi_{2n-1}^{(n)}w_{10}, \tag{A.17}$$

where $\Phi_k^{(n)}$ are functions of $F(x)$ and its derivatives.

$$w_{10} = \sqrt{\frac{2}{K}}\left(\frac{K}{2}\frac{\partial w_0}{\partial x} + F(x)w_0\right). \tag{A.18}$$

Substituting

$$w_1 = \sum_{n=0}^{\infty}\epsilon^{2n}w_{1n} \tag{A.19}$$

into Eq. (A.12) and using the fact that

$$w(x,t) = \int_{-\infty}^{\infty} w(x,y,t)\,\mathrm{d}y = w_0(x,t),$$

we obtain the following equation for $w(x,t)$:

$$\frac{\partial w}{\partial t} = \sqrt{\frac{K}{2}}\sum_{n=0}^{\infty}\epsilon^{2n}\frac{\partial w_{1n}}{\partial x}. \tag{A.20}$$

If ϵ^2 is sufficiently small then the series (A.19) is converged and Eq. (A.20) is the exact one-dimensional equation for the probability density $w(x,t)$.

In a stationary case Eq. (A.20) becomes

$$\sqrt{\frac{K}{2}}\sum_{n=0}^{\infty}\epsilon^{2n}w_{1n} = -G, \tag{A.21}$$

where G is the probability flux. In this case the derivatives of w_{10}, which are contained in the expressions for w_{1n}, in their turn should be expanded as power series in ϵ^2

$$\frac{\partial w_{10}}{\partial x} = -\epsilon^2\left[F''(x) + \epsilon^2\left(\frac{3K}{4}F^{IV}(x) + 2F(x)F'''(x) + 6F'(x)F''(x)\right) + \cdots\right]w_{10},$$

$$\frac{\partial^2 w_{10}}{\partial x^2} = -\epsilon^2\left[F'''(x) + \epsilon^2\left(\frac{3K}{4}F^V(x) + 2F(x)F^{IV}(x) + 8F'(x)F'''(x) + 6(F''(x))^2\right) + \cdots\right]w_{10}.$$

Appendix B. Integral expressions

We use the following denotations:

$$F[f(x)] = \int_0^L f(x)\exp\left(\frac{2(U(x)-\varphi x)}{K}\right)\mathrm{d}x,$$

$$FF[f(x')] = \int_0^L \int_0^x f(x')\exp\left(\frac{2(U(x')-U(x)-\varphi(t)(x'-x))}{K}\right)\mathrm{d}x'\,\mathrm{d}x,$$

$$f_1(x) = \frac{3K}{4}f'''(x) + 2f(x)f''(x) + (f'(x))^2,$$

$$f_2(x) = \frac{29K^2}{48}f^V(x) + \frac{K}{8}\left(23f(x)f^{IV}(x) + 52f'(x)f'''(x) + 31(f''(x))^2\right) + \frac{7}{2}f^2(x)f'''(x) + 12f(x)f'(x)f''(x) + 2(f'(x))^3,$$

$$f_3(x) = \frac{23K}{8}f^{IV}(x) + 7f(x)f'''(x) + 12f'(x)f''(x),$$

$$f_4(x) = \frac{143K^3}{288}f^{VII}(x) + \frac{K^2}{144}\left(485f(x)f^{VI}(x) + 1677f^V(x)f'(x) + 3081f^{IV}(x)f''(x) + 1820(f'''(x))^2\right) + \frac{K}{16}(123f^2(x)f^V(x) + 713f(x)f^{IV}(x)f'(x) + 1147f(x)f'''(x)f''(x) + 760f'''(x)(f'(x))^2 + 919(f''(x))^2f'(x)) + \frac{71}{12}f^3(x)f^{IV}(x) + \frac{83}{2}f^2(x)f'''(x)f'(x) + \frac{129}{2}f(x)f''(x)(f'(x))^2 + \frac{105}{4}f^2(x)(f''(x))^2 + 5(f'(x))^4,$$

$$f_5(x) = \frac{485K^2}{144} + \frac{123K}{8}f(x)f^V(x) + \frac{K}{16}(713f^{IV}(x)f'(x) + 1147f'''(x)f''(x)) + \frac{71}{4}f^2(x)f^{IV}(x) + 83f(x)f'''(x)f'(x) + \frac{129}{2}f''(x)(f'(x))^2 + \frac{105}{2}f(x)(f''(x))^2,$$

$$f_6(x) = \frac{123K}{8}f^V(x) + \frac{71}{4}f(x)f^{IV}(x) + \frac{83}{2}f'''(x)f'(x) + \frac{105}{4}(f''(x))^2.$$

Using these notations we have

$$I_4(\varphi) = F[f'(x)],\quad I_7(\varphi) = F[2f''(x)],\quad I_6(\varphi) = F[f_1(x)],\quad I_{12}(\varphi) = F[f_2(x)],\quad I_{13}(\varphi) = F[f_3(x)],$$

$$I_{14}(\varphi) = F\left[\frac{7}{2}f'''(x)\right],\quad I_{18}(\varphi) = F[f_4(x)],\quad I_{19}(\varphi) = F[f_5(x)],\quad I_{20}(\varphi) = F[f_6(x)],$$

$$I_{21}(\varphi) = F\left[\frac{71}{12}f^{IV}(x)\right],$$

and for double integrals

$$I_5(\varphi) = FF[f'(x')],\ I_8(\varphi) = FF[f_1(x')],\ I_9(\varphi) = FF[2f''(x')],\ I_{15}(\varphi) = FF[f_2(x')],$$

$$I_{16}(\varphi) = FF[f_3(x')],\ I_{17}(\varphi) = FF\left[\frac{7}{2}f'''(x')\right],\ I_{22}(\varphi) = FF[f_4(x')],\ I_{23}(\varphi) = FF[f_5(x')],$$

$$I_{24}(\varphi) = FF[f_6(x')],\ I_{25}(\varphi) = FF\left[\frac{71}{12}f^{IV}(x)\right].$$

References

[1] Peskin C, Odell G, Oster G. Cellular motions and thermal fluctuations: the Brownian ratchet. Biophys J 1993;65:316–24.
[2] Svoboda K, Schmidt CF, Schnapp BJ, Block SM. Direct observation of kinesin stepping by optical trapping interferometry. Nature 1993;365:721–7.
[3] Magnasco MO. Forced thermal ratchets. Phys Rev Lett 1993;71:1477–81.
[4] Astumian RD, Bier M. Fluctuation driven ratchets: molecular motors. Phys Rev Lett 1994;72:1766–9.
[5] Doering CR. Randomly rattled ratchets. Nuovo Cimento Soc Ital Fiz 1995;17D:685–97.
[6] Astumian RD, Bier M. Mechanochemical coupling of the motion of molecular motors to ATP hydrolysis. Biophys J 1996;70: 637–53.
[7] Hänggi P, Bartussek R. Brownian rectifiers: how to convert Brownian motion into directed transport. In: Parisi J, Müller SC, Zimmermann W, editors. Nonlinear physics of complex systems. Current status and future trends. Berlin: Springer; 1996. p. 294–308.
[8] Jülicher F, Ajdari A, Prost J. Modeling molecular motors. Rev Mod Phys 1997;69:1269–81.
[9] Bier M. Brownian ratchets in physics and biology. Cont Phys 1997;38:371–80.
[10] Landa PS. Noise-induced transport of Brownian particles with consideration for their mass. Phys Rev E 1998;58:1325–33.
[11] Faucheux LP, Bourdieu LS, Kaplan PD, Libchaber AJ. Optical thermal ratchet. Phys Rev Lett 1995;74:1504–7.
[12] Ajdari A, Prost J. Movement induit par un potential de basse symétrie: dielectrophorése pulsée. C R Acad Sci Paris 1992;315:1635–9.
[13] Gorre-Talini L, Spatz JP, Silberzan P. Dielectrophoretic ratchets. Chaos, Soliton & Fractals 1998;8:650–6.
[14] Feynman RP, Leighton RB, Sands M. The Feunman lectures on physics, vol. 1. Reading (MA): Addison-Wesley, Palo Alto, London, 1963 [chapter 46].
[15] Millonas M, Dykman MI. Transport and current reversal in stochastically driven ratchets. Phys Lett A 1994;185:65–9.
[16] Bier M. Reversals of noise-induced flow. Phys Lett A 1996;211:12–8.
[17] Bartussek R, Hänggi P, Lindner B, Schimansky-Geier L. Ratchets driven by harmonic and white noise. Physica D 1997;109:17–23.
[18] Lindner B, Schimansky-Geier L, Reimann P, Hänggi P, Nagaoka M. Inertia ratchets: a numerical study versus theory. Phys Rev E 1999;59:1417–24.
[19] Landa PS, McClintock PVE. Changes in the dynamical behaviour of nonlinear systems induced by noise. Phys Rep 2000;323:1–80.
[20] Jung P. Periodically driven stochastic systems. Phys Rep 1993;234:176.
[21] Blekhman II. In: Vibrational Mechanics. Moscow: Nauka; 1994 [in Russian].
[22] Bartussek R, Hänggi P, Kissner JG. Periodically rocked thermal ratchets. Europhys Lett 1994;28:459–64.
[23] Stratonovich RL. In: Topics in the theory of random noise, vol. 1. New York: Gordon and Breach; 1963.
[24] Stratonovich RL. In: Topics in the theory of random noise, vol. 2. New York: Gordon and Breach; 1967.